

Determination of Optimum Steering Trailing Arm Angle for a 3-Wheel HPV

By Timothy J. Gorman

Abstract

The purpose of this investigation is to develop a mathematical model for determining the desired angle of steering trailing arms with respect to the steered wheels' primary axle in three-wheeled vehicles. This angle will minimize tire "scrub", or the forced sideslip through the turn. It was also necessary to quantify the amount of power loss in a system whose trailing arms in their unturned state are parallel to the central vehicle plane, thereby justifying the need for this accommodation. In both cases, mathematical models were developed to describe the geometry of the vehicle's subsystems and their role in affecting the performance of the vehicle system as a whole. Approximate sample values were introduced for the descriptive variables in these equations to illustrate the salient points being made quantitatively. The results of the power loss calculations on our sample geometry yielded values in the most extreme cases of over 1.0 watts of power loss per steered wheel, amounting to potentially 1% of total power input. This indicates a definite need for some form of accommodation. The calculations for the geometry of a compensated system show that an optimum trailing arm angle does not practically exist, at least for the system analyzed here. Using the closest available value results in a steering angle 98% of optimum, compared with 93% in an uncompensated system, depending on the curve size. The benefits of and ease in determining and implementing this design modification are such that it should be considered by designers using a three-wheel configuration in their vehicles. In vehicles where even small amounts of energy loss are crucial (i.e., H.P.V.'s), this design characteristic may be essential, both for the benefits of energy savings and reduction in tire wear.

1.0 Optimized steering geometry.

Three wheeled vehicles have performance characteristics which are very different from vehicles with two or four wheels. Similarly, not all three wheelers are created equal. Each design has performance characteristics all it's own. A fairly conventional three-wheeled configuration is used here as a model to demonstrate optimal steering mechanism geometry. In this model, the steered wheels are on the front of the vehicle, with the driven wheel on the rear. The use of the reverse configuration, namely steering wheels rear and driven wheel forward, is not recommended without understanding the dynamics involved. Utilizing an appropriate compensation mechanism is required. Nonetheless, these equations will function in such a design. In either configuration, the steered wheels are mounted on two short secondary axles, with separate trailing arms, and pivot on vertical axes at A_L and A_R (see Figure 1.1). The distance between A_L and A_R is $2W_w + 2T$ (see Section 3.0 for the exact definition of the variables W_w and T). The wheelbase length is W_b . θ_{RT} and θ_{LT} represent the angles with respect to the driven wheel axle that the right and left steered wheel secondary axles, respectively, should attain in an optimally compensated system through a left-hand turn.

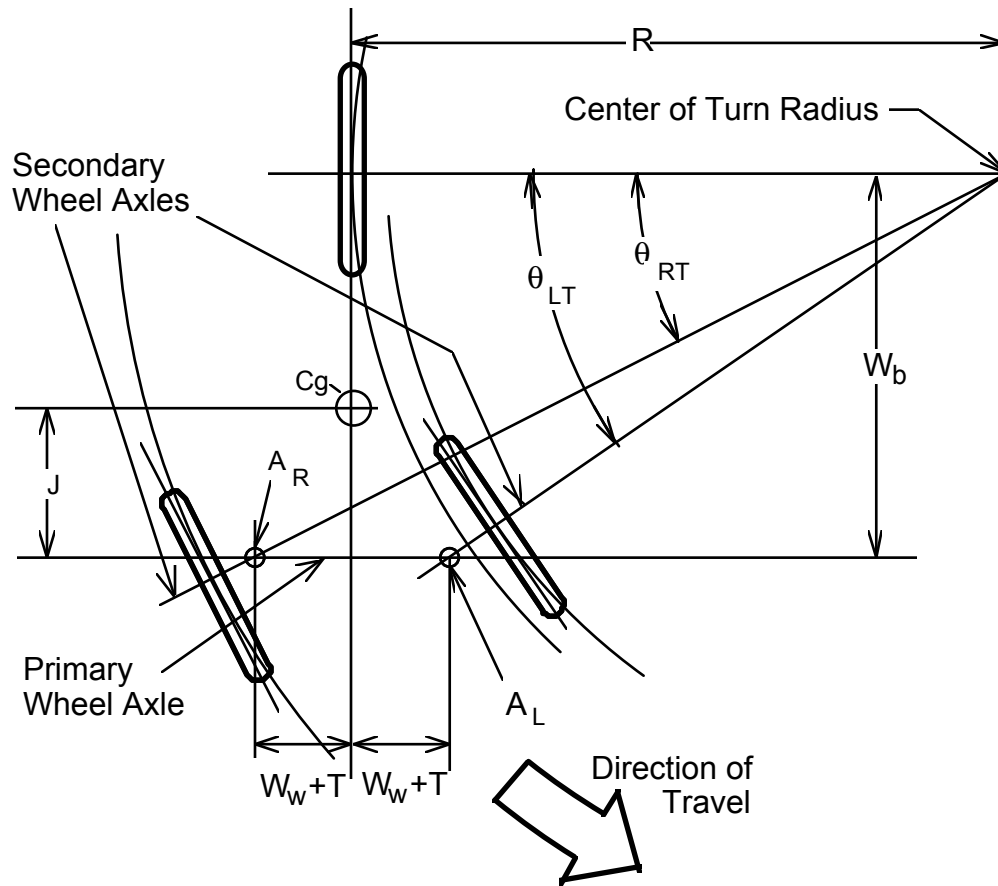


Figure 1.1: Geometric diagram for three-wheeled vehicle in a turn.

The ideal geometry will minimize "scrub". This is the tendency for the tire to slide sideways a small amount for each increment of distance traveled forward while in the turn. Negating such additional factors as overall sideslip, eliminating scrub requires that the plane of each wheel lie tangent to an arc whose center is the center for the curve of the road itself. Each of the three wheels would consequently lie tangent to concentric arcs, their axles pointing to this common center point, as in Figure 1.1. In essence, to minimize energy loss, the planes of the steered wheels need to "toe out" slightly. Otherwise, the result is a "snowplow" effect similar to what one does when stopping on skis. The angle of the wheel, with respect to the motion of the body mass, causes a certain component of the forward momentum to translate at a right angle to motion, and thus be lost through the heat of friction between the tire and the road. Isolating the outside (right) and inside (left) steering wheels, their optimum angles with respect to the central axis of the vehicle can be expressed in Equations 1.1 and 1.2. These formula are derived through simple trigonometric evaluation of the vehicle's geometry in the turn. Using sample values for the dimensions of a typical three-wheeler, we perform calculations of these formula for various turn radii. Figure 1.2 illustrates the relationship between these two angles through the

turn range. Clearly, there is a definite discrepancy between the optimum steering angle for each wheel, increasing as the turn radius decreases. In a system in which this difference is not compensated, the resulting geometric offset is made up in "scrub".

$$\theta_{RT} = \text{Arctan} \frac{W_b}{R + W_W + T}$$

Eq. 1.1: Optimum outside (right) wheel axle (left) wheel angle in turn.

$$\theta_{LT} = \text{Arctan} \frac{W_b}{R - W_W - T}$$

Eq. 1.2: Optimum inside axle angle in turn.

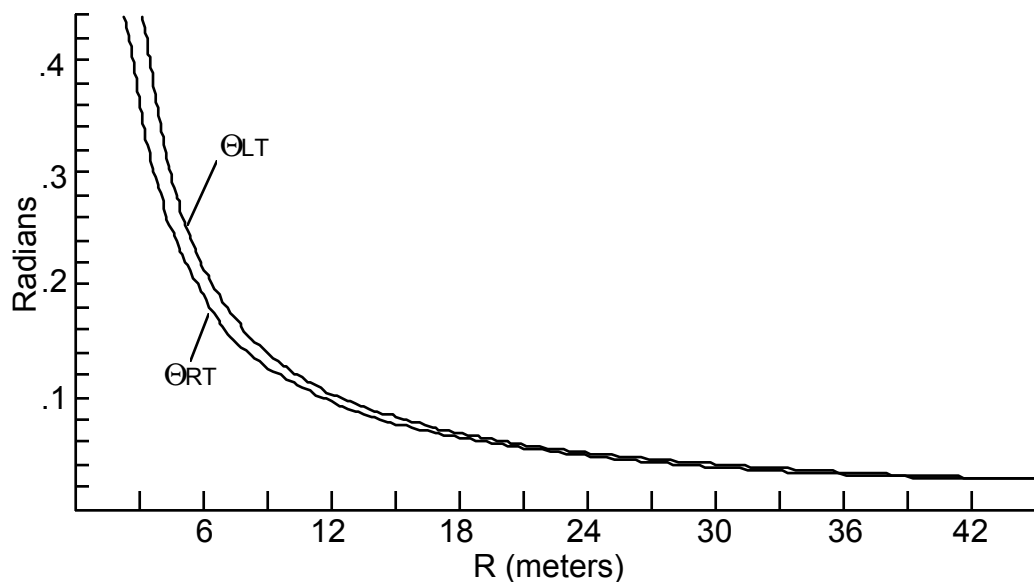
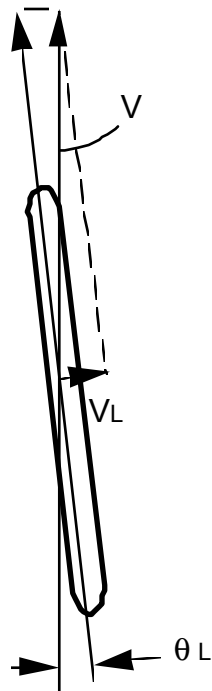


Figure 1.2: Plot of optimum outside (θ_{RT}) and inside (θ_{LT}) wheel angles.

2.0 Calculating power losses due to tire scrub.

The amount of power loss in a system whose trailing arms are perpendicular to the secondary axles of the steered wheels is determined by the "degree of scrub" (θ_D) for each wheel. θ_D can be defined as the angular offset between the optimal turn angle of a properly compensated system and that of a system whose wheels stay parallel to each other. In the uncompensated system, the distance between the points where the tie rods connect to the trailing arms remains the same throughout the turn. Energy is lost from the system through the lateral velocity vector V_L (see Figure 2.1). Calculating V_L requires that we know both the forward velocity V (in meters / second) and θ_D , according to the vector analysis in Equation 2.1. For each wheel, finding θ_D is a matter of determining the difference between the optimum wheel angle and that achieved with perpendicular trailing arms, using Equation 2.2. This equation assumes that the total angular differential will be evenly distributed between both steered wheels, and automatically establish an equal θ_D between them. Under realistic conditions,

this will necessarily not always be the case. However, as one wheel establishes a more optimal line, reducing scrub, the other will always go farther away, increasing scrub losses by a comparable amount. This equation may not model the system for all possible variations in left-to-right wheel angle deviation, but will be adequate for the purpose of this investigation. A rough assessment of the total power loss in the entire system is the quantity sought.



$$V_L = V \sin \theta_D$$

Fig. 2.1: Force resolution diagram for uncompensated wheel.

Eq. 2.1: Vector analysis of wheel lateral velocity.

$$\theta_D = \frac{\theta_{LT} - \theta_{RT}}{2}$$

Eq. 2.2: Equation for determining "degree of scrub" (θ_D).

The quantity of power loss per steered wheel can be estimated through the use of the base Equation 2.3. This calculation assumes no resistance to motion, and thus no power loss, in any force vector which proceeds in the plane of the wheel. The velocity vector perpendicular to the plane, V_L , will attempt to drag the wheel sideways. This friction-generating vector multiplied by the force required to drag the tire against the pavement gives us the power lost through this vector, in watts. The frictional force is determined by the proportion of the normal force M on each steered wheel, in kilograms, converted to Newtons and multiplied by the sliding frictional coefficient of rubber against pavement, μ_k . The value of M is determined through the application of Equation 2.4, which analyzes the distribution of the entire vehicle and rider mass over the three wheels by the location of the center of gravity of the whole. Equation 2.3 does not take into

account weight distribution factors which may be generated through centrifugal forces and body roll in the turn. It is assumed that as weight increases over one wheel, it will decrease comparably on the other, equalizing the full-system value. Nor does it accommodate such variability caused by swerving or wheel wobble. Rather, it gives us an averaged approximation, as if these forces were not present. For the purpose of these calculations, this will be adequate. More precise evaluation of these other forces become more crucial in the more detailed aspects of steering system design.

$$P_L = \frac{M\mu_k V_L}{9.81}$$

Equation 2.3: Total single wheel power loss (in watts) by uncompensated turned wheels. M= wheel load (Kg). vehicle (Kg).

μ_k = coefficient of sliding friction.

$$M = \frac{W_b M_T - W_b J}{2W_b}$$

Equation 2.4: Calculation of individual wheel load for three-wheeled vehicle. M_T =weight of

J = distance from steered wheel axle to center of gravity. W_b = wheelbase length.

To arrive at a general equation for power loss, we first incorporate Equations 1.1 and 1.2 into Equation 2.2, and Equation 2.2 into 2.1. We then incorporate the resultant along with Equation 2.4 into Equation 2.3 to arrive finally at Equation 2.5.

$$P_L = \frac{V\mu_k(W_b M_T - W_b J) \sin \frac{\text{Arctan} \frac{W_b}{R+W_w+T} - \text{Arctan} \frac{W_b}{R-W_w-T}}{2}}{19.62W_b}$$

Equation 2.5: General equation for power loss from uncompensated turned wheel (for both wheels, multiply by 2).

To analyze Equation 2.5, we introduce values descriptive of the geometry and weight of a typical 3-wheeled recumbent-type vehicle with rider (variables $W_b=1.07m$, $W_w+T=.46m$, $M_T=90kg$, and $J=.4m$). For the sliding frictional coefficient μ_k , an apparatus was constructed to measure the friction of a typical high pressure bicycle tire against concrete. This test yielded an average value of 1.2. A full analysis requires that we evaluate Equation 2.5 across a full range of both velocities and turn radii. The data in Table 2.1 gives the total power loss for each steered wheel and is shown graphically in Figure 2.2. From the data, it is apparent that power losses maximize at lower turn radius as well as increase with speed. This makes logical sense as, from the discussion in Section 1.0, the differential between optimum θ_R and θ_L also increases at lower radius. The values shown at very low radius and very high speed would in all likelihood never

occur, because the chances of there being a steering system which would allow this kind of dynamic turn are slim.

Radius (m)	Velocity (m/s)=							
	2	4	6	8	10	12	14	16
2	0.679	1.356	2.037	2.716	3.359	4.074	4.753	5.432
4	0.203	0.407	0.610	0.813	1.017	1.220	1.424	1.627
6	0.093	0.186	0.279	0.372	0.465	0.558	0.651	0.745
8	0.052	0.103	0.155	0.207	0.259	0.310	0.362	0.414
10	0.034	0.067	0.103	0.138	0.172	0.207	0.241	0.276
12	0.024	0.048	0.072	0.096	0.121	0.145	0.169	0.193
14	0.017	0.034	0.052	0.069	0.086	0.103	0.121	0.138
16	0.014	0.028	0.041	0.055	0.069	0.083	0.099	0.110
18	0.010	0.021	0.031	0.041	0.052	0.062	0.072	0.083

Table 2.1: Total power loss per steered wheel (watts) in turn from steering system with parallel trailing arms.

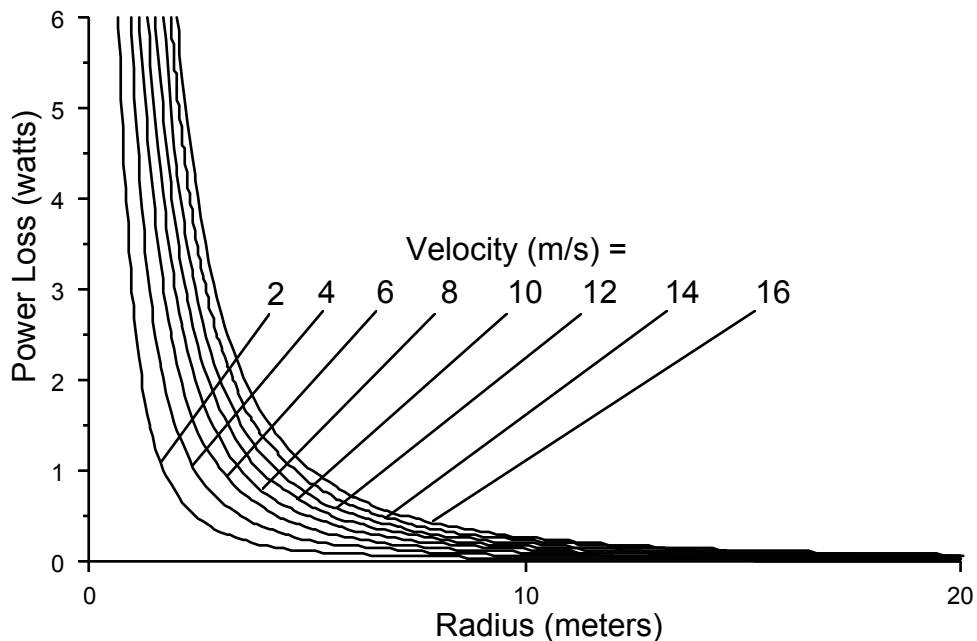


Figure 2.2: Plot of power loss for steered wheels of uncompensated steering system for various turn radii and velocities.

3.0 Calculating optimized trailing arm angle to minimize energy loss.

Modifying trailing arm angle is a common technique that has been used extensively in the design of vehicles to minimize the amount of energy loss from tire scrub in turns. Developing the proper mathematical model to describe this system and determine the optimum value is another matter. The methodology used here is presented in some detail as to permit duplication and adaptation to related projects.

Before proceeding with a mathematical analysis of this system, it is first necessary to understand the principle behind the solution. As was stated previously, minimizing drag necessarily requires that we minimize the potential difference between the optimum angle of each wheel plane, with respect to the curve, and the actual angle. From Figure 1.1, and from the data in Table 2.1, we've shown that as the outside (right) wheel establishes its turn angle, the inside (left) wheel's angle must be greater by a quantifiable degree. If the trailing arm which forces each wheel to rotate about the vertical pivot at AL and AR (see Figure 1.1) is perpendicular to each wheel's secondary axle, each wheel turns to the same degree. However, if this trailing arm is at some angle to the wheel's shaft other than perpendicular, each turns at a different rate. As each wheel rotates, the angle between each trailing arm and the tie rod which is controlling it gets closer to or further from 90 degrees. The wheel whose trailing arm is closer to 90 degrees to the tie rod will have a slower instantaneous rate of rotation at that point than the other.

Figure 3.1 shows a diagram of the geometric model which we will use to create our mathematical model. Before we create and analyze a mathematical model of our system, we will make no assumptions about whether our trailing arms should be angled inboard or outboard of the rotation points AR and AL , but in Figure 5 they are shown angled inboard. Neither will we make any other assumptions about what the optimum dimensions of the rest of the geometry will be. Therefore, our mathematical model must be made to accommodate a wide range of possible variations in geometry. For the sake of simplicity, we will only analyze the geometry for the condition of the tie rods and trailing arms being located forward of the steering wheels' axle. The calculation where this mechanism is located between the front and rear wheels is similar in concept. Furthermore, our calculations model our system on the assumption that the tie rods and trailing rods lie as well as articulate within a single plane. Finally, the equations model the system on the assumption that the tie rods are equal in length and translate horizontally to the left and right along a straight line as the means of translating force from the steering controls to the system. These calculations will accommodate the condition where force is translated through the use of a rack and pinion mechanism at the tie rod connections. Simply enter the dimension for half the rack length for the variable T .

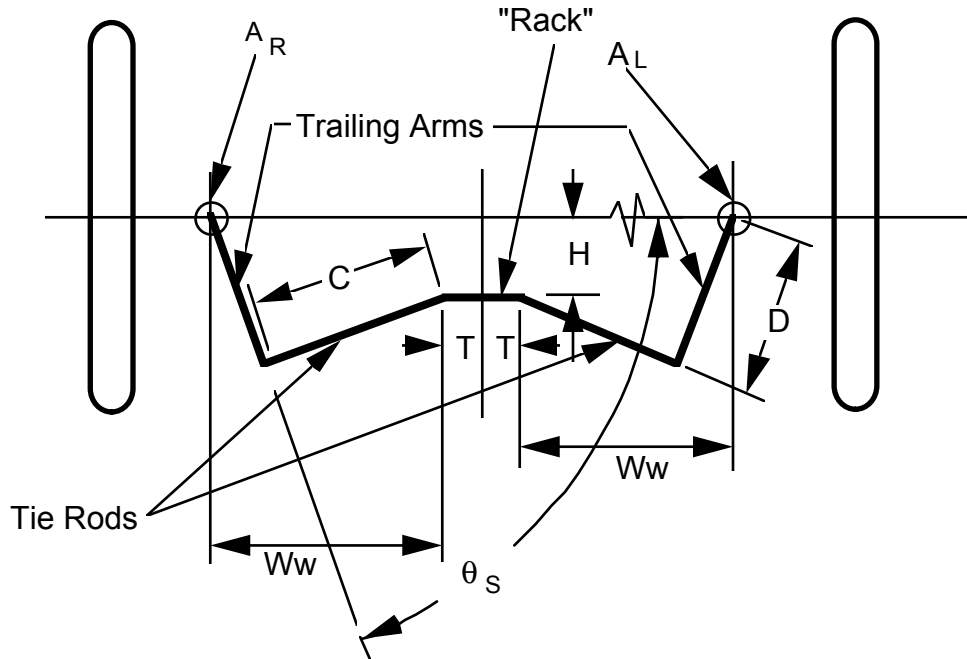


Figure 3.1: Steering mechanism geometry.

Calculating the optimum angle for the trailing arm must proceed through a number of steps. It is possible to derive a single formula to find the desired value but, having done this, it was found that no single optimal value for θ_s exists. Furthermore, it would deny us the opportunity to check our accuracy as well as the legitimacy of our process. Though we may derive useful values as the end product of such an equation, it does us little good if values for interim variables are fictitious in a practical sense. Despite the fact that numbers don't lie, it must not be forgotten that these numbers represent real dimensions and angles on a potentially viable vehicle design.

First, we calculate the length of the tie rod for some described geometry. In order to cover a wide range of possible variations, we analyze the straight-wheel geometry as one of two four-bar linkages whose sides are D , Ww , H and C . This quadrilateral is then treated as two triangles sharing a common side. This line segment, if it could be seen, would pass from the center of the vehicle at the intersection of the primary axle to the connection point of the tie rod and trailing arm. The law of cosines is used to define the characteristics of these two triangles, resulting in Equation 3.1.

$$C = \sqrt{D^2 + Ww^2 - 2DWw \cos \theta_s + H^2 - 2HD \sin \theta_s}$$

Equation 3.1: Length of tie rod (C) based on trailing arm length (D), distance from central tie rod connection to vertical pivot (Ww), distance from central tie rod connection to primary wheel axis (H), and initial trailing arm angle (θ_s).

Second, we must isolate the optimum angle which the right wheel axle must establish through a left-hand turn. This formula is based on Equation 1.1, modified to reflect the trailing arm angle rather than the individual steered wheel axle. The characteristic angle used, $\theta_{R(opt)}$, is the new angle established between the right trailing arm and the primary wheel axle in the turn, as shown in Figure 3.2. This is a simple right triangle solution which results in Equation 3.2.

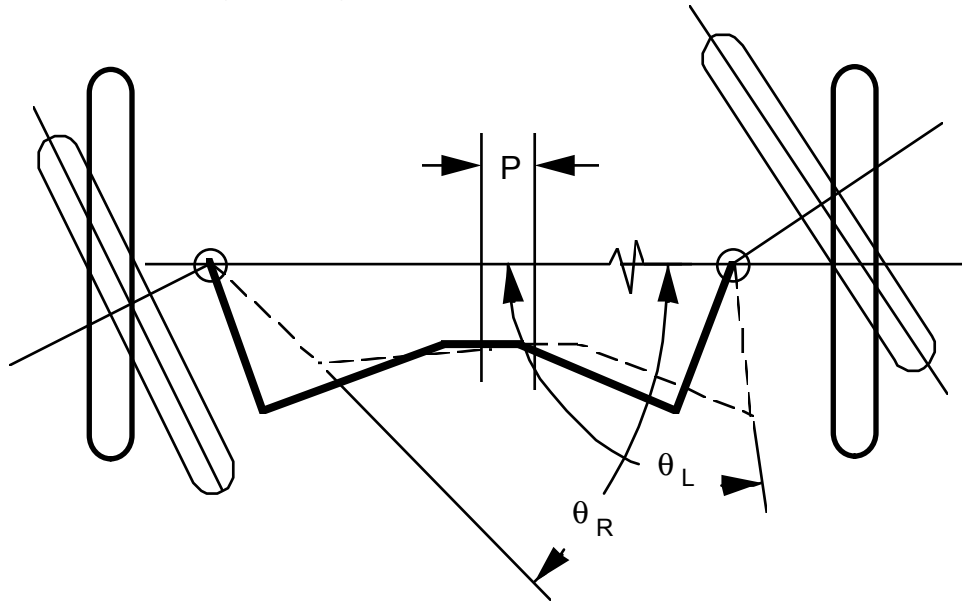


Figure 3.2: Left and right side wheel rotation in left turn.

$$\theta_{R(opt)} = \theta_S - \text{atan} \frac{W_B}{R + W_W + T}$$

Equation 3.2: Optimum characteristic right trailing arm angle ($\theta_{R(opt)}$) based on initial trailing arm angle (θ_S), radius of curve to central plane of vehicle (R), distance from central tie rod connection to vertical pivot A_R (W_W), wheelbase length (W_B), tie rod length (C), and half rack length (T).

Our third step involves the calculation to find the lateral offset P of the central tie rod connecting point(s) when the vehicle makes its turn (see Figure 3.2). The process of deriving this calculation is similar to that done to establish Equation 3.1. In this case, we analyze only the right-hand side quadrilateral's change in shape as the wheel turns, as reflected in the change in length of the same diagonal. The quadratic equation is then utilized to solve for P , yielding Equation 3.3.

$$P = D \cos \theta_{R(opt)} - W_W + .5 \sqrt{(2W - 2D \cos \theta_{R(opt)})^2 - 4(H^2 - C^2 + D^2 + W^2 - 2DW \cos \theta_{R(opt)} - 2HD \sin \theta_{R(opt)})}$$

Equation 3.3: Central tie rod connection lateral offset (P) based on trailing arm length (D), distance from central tie rod connection to vertical pivot AR (Ww), distance from central tie rod connection to primary wheel axle (H), and optimum characteristic right trailing arm angle($\theta_{R(opt)}$).

The fourth step requires that we calculate the reaction movement to the left side four-bar linkage that the offset P causes. This will determine the left side wheel rotation about AL. Once again, we use the 2-triangle methodology similar to that used in deriving Equation 3.1 and 3.3. We solve the resultant equality for our desired value, θ_L , through the use of the quadratic equation. By this we arrive at Equation 3.4.

$$\theta_L = A \sin \frac{C^2 - D^2 - (W_W - P)^2 - H^2 - 2D(W_W - P) \sqrt{\frac{W_W - P}{H}^2 - \frac{C^2 - D^2 - (W_W - P)^2 - H^2}{-2HD}} + 1}{-2HD \frac{W_W - P}{H} - 2HD}$$

Equation 3.4: Reaction rotation of left side wheel (θ_L) based on trailing arm length (D), distance from central tie rod connection to vertical pivot AL (Ww), distance from central tie rod connection to primary wheel axis (H), tie rod length (C), and central tie rod connection lateral offset (P).

Finally, we must find out what the optimum left wheel rotation $\theta_{L(opt)}$ should be so that we can compare it with the values derived from the analysis of Equation 3.4. Equation 3.5 gives us this value. Like Equation 3.2, it is a right triangle solution of the steered wheel's geometry in the turn, but is based on Equation 1.2 rather than Equation 1.1.

$$\theta_{L(opt)} = \theta_S + A \tan \frac{W_B}{R - W_W - T}$$

Equation 3.5: Optimum characteristic left trailing arm angle ($\theta_{L(opt)}$) based on initial trailing arm angle (θ_S), radius of curve to central plane of vehicle (R), distance from central tie rod connection to rotational axis AL (Ww), wheelbase length (WB), and half rack length (T).

4.0 Analysis of optimization calculations

A full assessment of this system requires that we cover a broad spectrum of possible solutions for trailing arm angles. This not only provides us with the

greatest opportunity of finding a solution but also a better idea of what is happening dynamically with variations in geometry. For our ultimate goal, namely finding the optimum trailing arm angle θ_s , we will choose a range from .8 radians (45.8 degrees) to 2.6 radians (149 degrees). With any luck, our solution will fall within this range, for outside of it we run the risk of two problems. First, we might run out of available rotation room. As the inside (left) wheel rotates, the trailing arm gets closer to parallel to the tie rod pushing on it. When this state is reached, the wheel assembly will not rotate any further. Second, it may become too difficult to steer. The momentum of the vehicle traveling along a straight path attempts to keep it moving along that path. Steering the vehicle involves imparting some lateral force on the road surface which will cause the mass of the vehicle to deviate from that straight line. This force is transferred from the driver's arms through the steering controls to the steering mechanism and finally to the wheels. The trailing arm length provides a certain amount of torque around the vertical pivots A_R and A_L and an inordinately large or small trailing arm angle reduces the effective length of this moment arm. The consequent effect would be an increased component of the force of the road being translated to the driver's arms. The actual quantity of this force and the amount which is allowable is the subject of a different paper, but suffice it to say, it is a consideration which should have some bearing on the final configuration which is used.

The wide range of possible solutions for θ_s should also be assessed over a wide range of possible curve radii. This would ensure that the solution which we arrive at will operate effectively through the full range of wheel turn. Furthermore, it would give us an adequate representation of the dynamic functionality of all the components in the system at the extremes of motion. We will use a range from 200 cm (a sharper curve than a tight right-hand urban corner) to 3000 cm. The latter value is not the greatest radius one might encounter, but as we will see, when steering around very gradual turns of higher radius, the amount of wheel assembly rotation is so minute that trailing arm angle makes little difference towards accommodation.

Table 4.1 gives solutions for tie rod length C in a sample steering system, calculated using Equation 3.1, across the full range of θ_s . In this steering system, W_w (tie rod lateral dimension) = 46 cm, W_b (wheelbase dimension) = 107 cm, D (trailing arm length) = 12 cm, T (half "rack" length) = 0, and H ("rack" to primary wheel axle dimension) = 12 cm. Also in Table 4.1 are values for the optimal right wheel assembly rotation $\theta_{R(opt)}$, calculated using Equation 3.2, through both our θ_s and R (curve radius) ranges. These values for C and $\theta_{R(opt)}$ are used in Equation 3.3 to arrive at the values for P in Table 4.2. It should be noted that the table position for values of P in Table 4.2 correspond to the table position for values of $\theta_{R(opt)}$ in Table 4.1 used in the calculation. Likewise, these values for P and those for C in Table 4.1 are used in Equation 3.4 to calculate values for θ_L found in Table 4.3. Finally, we use Equation 3.5 to calculate the values for $\theta_{L(opt)}$ in Table 4.4.

θ_s (rad)	C (cm)	$\theta_{R(opt)}$ (rad) for $R=$ (cm)					
		200	400	700	1000	2000	3000

0.8	37.79	0.39	0.57	0.66	0.70	0.75	0.77
1.0	39.56	0.59	0.77	0.86	0.90	0.95	0.97
1.2	41.66	0.79	0.97	1.06	1.10	1.15	1.17
1.4	43.96	0.99	1.17	1.26	1.30	1.35	1.37
1.6	46.35	1.19	1.37	1.46	1.50	1.55	1.57
1.8	48.73	1.39	1.57	1.66	1.70	1.75	1.77
2.0	51.01	1.59	1.77	1.86	1.90	1.95	1.97
2.2	53.11	1.79	1.97	2.06	2.10	2.15	2.17
2.4	54.99	1.99	2.17	2.26	2.30	2.35	2.37
2.6	56.58	2.19	2.37	2.46	2.50	2.55	2.57

Table 4.1: Numerical data from Equations 3.1 and 3.2.

θ_s	P (cm) for R=					
	200	400	700	1000	2000	3000
0.8	2.15	1.51	1.00	0.74	0.39	0.27
1.0	3.17	2.04	1.30	0.95	0.49	0.34
1.2	3.96	2.44	1.52	1.10	0.57	0.39
1.4	4.50	2.69	1.65	1.19	0.61	0.41
1.6	4.80	2.80	1.70	1.22	0.62	0.42
1.8	4.89	2.80	1.68	1.21	0.61	0.41
2.0	4.78	2.69	1.61	1.15	0.58	0.39
2.2	4.50	2.49	1.47	1.05	0.53	0.35
2.4	4.10	2.23	1.31	0.93	0.47	0.31
2.6	3.57	1.91	1.10	0.78	0.39	0.26

Table 4.2: Numerical data from Equation 3.3.

θ_s	θ_L for R=					
	200	400	700	1000	2000	3000
0.8	1.038	0.973	0.918	0.889	0.848	0.833
1.0	1.295	1.195	1.127	1.094	1.049	1.034
1.2	1.539	1.412	1.333	1.297	1.251	1.235
1.4	1.777	1.625	1.538	1.5	1.451	1.435
1.6	2.013	1.836	1.742	1.702	1.652	1.635
1.8	2.251	2.048	1.946	1.905	1.853	1.836
2.0	2.494	2.260	2.151	2.107	2.054	2.036
2.2	2.750	2.471	2.354	2.308	2.253	2.235
2.4	3.064	2.691	2.561	2.512	2.455	2.436
2.6	**	2.921	2.767	2.714	2.654	2.636

Table 4.3: Numerical data from Equation 3.4 (** no solution).

θ_s	θ_L (opt) for R=					
	200	400	700	1000	2000	3000
0.8	1.41	1.29	0.96	0.91	0.86	0.84
1.0	1.61	1.49	1.16	1.11	1.06	1.04
1.2	1.81	1.69	1.36	1.31	1.26	1.24
1.4	2.01	1.89	1.56	1.51	1.46	1.44
1.6	2.21	2.09	1.76	1.71	1.66	1.64
1.8	2.41	2.29	1.96	1.91	1.86	1.84
2.0	2.61	2.49	2.16	2.11	2.06	2.04
2.2	2.81	2.69	2.36	2.31	2.26	2.24
2.4	3.01	2.89	2.56	2.51	2.46	2.44
2.6	3.21	3.09	2.76	2.71	2.66	2.64

Table 4.4: Numerical data from Equation 3.5.

Isolating the desired solution for θ_L is a matter of comparing the values from Table 4.3 with those in Table 4.4. Where corresponding positions in the two tables have values which are similar, the value for θ_s is most optimum for that curve radius. For this sample steering system configuration, a value of 2.4 for θ_s is closest to optimum. One might notice that at higher turn radius, there is little variation between the optimum and reaction values for θ_L . As previously mentioned, steering system accommodation has little effect because steered wheel angle deviation in the turn is so slight.

4.0 Conclusions

Results from the analysis of energy loss indicate that the amount is significant enough to merit the use of some design modifications to compensate. When turn radii are small, power losses can amount to as much as 1 watt per steered wheel. In a human powered vehicle operating on around 200 watts, this amount of power loss is potentially 1% of the total output. At higher radii, power losses are measurable, if small. Even if this energy loss is intermittent, in such a relatively low-powered system, any power losses which can be avoided should be.

The calculations presented for use in determining trailing arm angle indicate that a single, optimum trailing arm angle may or may not exist for all turn radii for a particular steering system configuration. For this example, an angle of 2.4 radians (137.5 degrees) was arrived at, though a value of somewhat less (2.3 radians) would be more optimal and can be determined either through interpolation of the existing data or through a subsequent calculation. At this angle, wheel rotation is approximately 98% of optimal, as opposed to 93% for an uncompensated system (corresponding to a value of 1.8 in Tables 4.3 and 4.4).